



## ARTICLE

# FIH-1-modulated HIF-1 $\alpha$ C-TAD promotes acute kidney injury to chronic kidney disease progression via regulating KLF5 signaling

Zuo-lin Li<sup>1</sup>, Bin Wang<sup>1</sup>, Lin-li Lv<sup>1</sup>, Tao-tao Tang<sup>1</sup>, Yi Wen<sup>1</sup>, Jing-yuan Cao<sup>1</sup>, Xiao-xiao Zhu<sup>1</sup>, Song-tao Feng<sup>1</sup>, Steven D. Crowley<sup>2</sup> and Bi-cheng Liu<sup>1</sup>

Incomplete recovery from episodes of acute kidney injury (AKI) can predispose patients to develop chronic kidney disease (CKD). Although hypoxia-inducible factor-1 $\alpha$  (HIF-1 $\alpha$ ) is a master regulator of the response to hypoxia/ischemia, the role of HIF-1 $\alpha$  in CKD progression following incomplete recovery from AKI is poorly understood. Here, we investigated this issue using moderate and severe ischemia/reperfusion injury (I/RI) mouse models. We found that the outcomes of AKI were highly associated with the time course of tubular HIF-1 $\alpha$  expression. Sustained activation of HIF-1 $\alpha$ , accompanied by the development of renal fibrotic lesions, was found in kidneys with severe AKI. The AKI to CKD progression was markedly ameliorated when PX-478 (a specific HIF-1 $\alpha$  inhibitor, 5 mg·kg<sup>-1</sup>·d<sup>-1</sup>, i.p.) was administered starting on day 5 after severe I/RI for 10 consecutive days. Furthermore, we demonstrated that HIF-1 $\alpha$  C-terminal transcriptional activation domain (C-TAD) transcriptionally stimulated KLF5, which promoted progression of CKD following severe AKI. The effect of HIF-1 $\alpha$  C-TAD activation on promoting AKI to CKD progression was also confirmed in vivo and in vitro studies. Moreover, we revealed that activation of HIF-1 $\alpha$  C-TAD resulted in the loss of FIH-1, which was the key factor governing HIF-1 $\alpha$ -driven AKI to CKD progression. Overexpression of FIH-1 inhibited HIF-1 $\alpha$  C-TAD and prevented AKI to CKD progression. Thus, FIH-1-modulated HIF-1 $\alpha$  C-TAD activation was the key mechanism of AKI to CKD progression by transcriptionally regulating KLF5 pathway. Our results provide new insights into the role of HIF-1 $\alpha$  in AKI to CKD progression and also the potential therapeutic strategy for the prevention of renal diseases progression.

**Keywords:** acute kidney injury; chronic kidney disease; renal fibrosis; HIF-1 $\alpha$  C-terminal activation domain; KLF5; FIH-1; PX-478

*Acta Pharmacologica Sinica* (2021) 42:2106–2119; <https://doi.org/10.1038/s41401-021-00617-4>

## INTRODUCTION

Acute kidney injury (AKI) is considered a major public health concern associated with high morbidity and mortality. Accumulating evidence indicates that the severity of AKI predicts subsequent progression to chronic kidney disease (CKD) [1, 2]. Mild/moderate AKI triggers intrinsic repair mechanisms that result in functional recovery from renal dysfunction, while individuals with severe AKI usually fail to recover from renal dysfunction and quickly progress to CKD [3, 4]. However, the exact mechanism remains poorly understood. Hypoxia, a common cause of kidney injury, is a critical instigator in the pathophysiology of AKI and its progression to CKD [5]. Compelling evidence indicates that the severity of hypoxia determines the outcome of AKI [6, 7]. Moreover, targeting hypoxia is a promising strategy for blocking the progression of kidney injury [8]. Therefore, it is of great clinical significance to investigate the exact mechanisms of hypoxia-dependent kidney injury progression.

Packed with mitochondria and dependent on oxidative phosphorylation, the proximal tubule is particularly vulnerable to ischemic/hypoxic insults. Failed tubule recovery is a critical pathological feature of severe AKI and a key initiator of

consequent CKD [9]. Importantly, the severity of proximal tubule injury has also been found to be correlated with renal prognosis [10]. Recent studies have shown that the renal tubule is a strong driving force for CKD progression after AKI by acting as inflammatory and fibrogenic cells [11]. However, the exact molecular mechanism of these actions remains to be elucidated.

Hypoxia-inducible factor-1 (HIF-1), comprising an inducible  $\alpha$  subunit (HIF $\alpha$ , the main hypoxia sensitive component) and a constitutively expressed  $\beta$  subunit (HIF $\beta$ ), is a key transcription factor that regulates adaptive responses to hypoxia. The oxygen-sensitive signal that controls HIF-1 activity is generated by a series of regulatory enzymes, namely, prolyl hydroxylases [PHDs, which hydroxylate specific prolyls (Pro402 and Pro564) in the NH<sub>2</sub>-terminal activation domain (N-TAD)] and factor-inhibiting HIF-1 [FIH-1, which hydroxylates a specific asparaginyl (Asn803) in the COOH-terminal activation domain (C-TAD)] [12]. Functionally, FIH-1 blocks the interaction of the HIF- $\alpha$  C-TAD with the transcriptional coactivator protein CREB-binding protein/p300, leading to the inactivation of the C-TAD. Importantly, a set of hypoxic genes are only regulated by FIH-1-controlled C-TAD. Thus, the bifunctional transcriptional character of HIF is controlled by N-TAD and C-TAD

<sup>1</sup>Institute of Nephrology, Zhongda Hospital, Southeast University School of Medicine, Nanjing 210009, China and <sup>2</sup>Division of Nephrology, Department of Medicine, Duke University, Durham VA Medical Centers, Durham, NC, USA

Correspondence: Bin Wang (wangbinhewei@126.com) or Bi-cheng Liu (Liubc64@163.com)

Received: 22 October 2020 Accepted: 17 January 2021

Published online: 3 March 2021

based on their sensitivity to FIH-1 expression. In response to hypoxia, HIF-1 $\alpha$  is expressed predominantly in the tubules and works as a master regulator of hypoxic stress. Activation of HIF-1 has strong renoprotective effects in AKI [13, 14], whereas inappropriate activation of HIF-1 $\alpha$  in tubules promotes the progression of kidney diseases, as evidenced by genetic and pharmacological modulation in animal models [15, 16]. Moreover, our previous study also found that HIF-1 $\alpha$  in tubules promotes kidney injury via epigenetic mechanisms [17]. These findings strongly suggest a dual role for HIF-1 $\alpha$  in kidney injury. However, the potential effect of HIF-1 $\alpha$  on AKI to CKD progression remains unclear.

In the present study, we clarified the role of HIF-1 $\alpha$  in the AKI to CKD transition using moderate and severe AKI models induced by ischemia/reperfusion injury (I/RI). We demonstrated that activation of the HIF-1 $\alpha$  C-TAD, which was modulated by FIH-1, was the determinative mechanism of AKI to CKD progression. Our study provides new insight into the role of HIF-1 $\alpha$  in driving the AKI to CKD transition and evidence for a novel therapeutic strategy for preventing renal disease progression.

## MATERIALS AND METHODS

### Ischemic AKI models

All animal experimental procedures were approved by the Ethics Review Committee for Animal Experimentation of Southeast University. Experiments were performed with 6–8-week-old male C57BL/6 mice (Vital River Laboratory Animal Technology Co., Ltd., Beijing, China). Mouse bilateral I/R injury models were established as previously described [6, 7, 18]. In brief, bilateral renal pedicles were clamped with artery clamps for 30 or 40 min to induce moderate or severe AKI, respectively. During the ischemic period, the mouse body temperature was maintained at ~36.5–37 °C using a temperature-controlled heating system. Sham control mice underwent the same surgical procedures without clamping of renal pedicles. Mice were killed under general anesthesia on day 1 or 14 after I/RI, and their serum and kidneys were harvested.

### In vivo PX-478 treatments, lentiviral transduction and KLF5-targeted siRNA administration

To inhibit HIF-1, beginning on day 5 after I/RI, mice were subjected to daily intraperitoneal injections of PX-478 (Selleck Chemicals LLC, Houston, TX, USA) or vehicle (PBS) at 5 mg/kg body weight for 10 consecutive days. For lentiviral gene transfer, lentiviruses expressing short-hairpin RNAs (shRNAs) targeting KLF5 (Lv-shKLF5) and negative control (Lv-shNC) were purchased from GenePharma (Shanghai, China). The shRNA targeting sequences were as follows: shKLF5, 5'-GCTCCCTCCAGTCCGATAAT-3', and shNC, 5'-TTCTCCGAACGTGTCACGT-3'. Lentiviruses expressing FIH-1 (Lv-FIH-1), the HIF-1 $\alpha$  C-TAD (Lv-HIF-1 $\alpha$  C-TAD) or negative control (Lv-NC), which contained the bHLH-PAS domain, were also purchased from GenePharma. Lv-mediated gene transfer in the kidneys of I/RI mice was performed by tail vein injection on day 3 and day 10 after I/R surgery ( $5 \times 10^8$  TU/mouse). The KLF5-targeted siRNA was transfected into mouse kidneys through tail vein injections by using in vivo-jetPEI reagent (Polyplus Transfection SA, New York, NY, USA) according to the manufacturer's instructions. Mice were euthanized on day 14 after I/RI. Serum and kidney tissues were collected for various analyses. The details of these methods are provided in the Supplementary Methods.

### Primary tubular epithelial cell and HK-2 cell culture

Kidneys were harvested from 6-week-old mice, and tubular epithelial cells (TECs) were isolated for primary culture using established methods [19]. The human proximal tubular epithelial cell line HK-2 was purchased from the American Type Culture Collection. Cells were cultured in DMEM-Ham's-F12 medium (HyClone, GE Healthcare Life Science, UT, USA) supplemented

with 10% fetal bovine serum and 1% penicillin-streptomycin (Gibco, Grand Island, NY, USA) in a humidified atmosphere of 5% CO<sub>2</sub> and 21% O<sub>2</sub> at 37 °C. Moderate or severe I/RI conditions in TECs were modeled in vitro. Administration of the PHD inhibitor FG-4592 [20] (Selleck Chemicals LLC, Houston, TX, USA) mimicked moderate I/RI conditions, and a combination of FG-4592 and FIH-1 inhibitor [N-oxalyl-D-phenylalanine (DM-NOFD) [21], D&C Chemicals, Shanghai, China] mimicked severe I/RI conditions [22]. Briefly, serum-starved cells were treated with FG-4592 (10  $\mu$ M) for 24 h, washed, and incubated under normal conditions for an additional 24 h, or serum-starved cells were treated with FG-4592 (10  $\mu$ M) + DM-NOFD (1 mM) continuously for 48 h.

### Plasmids, siRNA, and adenoviral transfection

For adenoviral (Ad) transfection, cells grown on chamber slides at 70% confluence were transduced with Ad-NC or Ad-FIH-1 for 24 h and then exposed to I/RI modeling conditions for 24 h. For plasmid transfection, cells were transfected with different plasmids using Lipofectamine 2000 (Invitrogen, USA) according to the manufacturer's instructions. For siRNA-mediated knock-down of KLF5, cells were transfected with 80 nM siRNA against human KLF5 (sense 5'-GCAGACUGCAGUGAAACAATT-3'; antisense 5'-UUGUUUCACUGCAGUCUGCTT-3') using Lipofectamine 2000 (Invitrogen, USA) according to the manufacturer's instructions. A sense scrambled control was used as a negative control.

### Nuclear and cytoplasmic protein extraction

Nuclear and cytoplasmic proteins were extracted using NE-PER™ Nuclear and Cytoplasmic Extraction Reagents (#78833, Thermo Scientific, USA) according to the manufacturer's instructions.

### Immunoprecipitation analyses

Cell preparation and immunoblotting (IB) analyses were performed as previously described [22]. Immunoprecipitation (IP) of HIF-1 $\alpha$  followed by IB analysis with an anti-FIH-1 antibody was performed with total cellular proteins from primary cultures using the Pierce™ Co-Immunoprecipitation Kit (#26149, Thermo Scientific, USA). Briefly, an anti-HIF-1 $\alpha$  antibody (Abcam) was first immobilized for 2 h using Aminolink Plus Coupling Resin. The resin was then washed and incubated for 12 h with 500  $\mu$ g cellular proteins extracted with RIPA buffer. The proteins were eluted using elution buffer and denatured with 5% 2-mercaptoethanol (#21985023, Thermo Scientific, USA). A negative control provided with the IP kit was used to assess nonspecific binding. The eluate was boiled at 95 °C for 10 min and loaded at 20  $\mu$ L per lane, and IB was performed to detect the levels of FIH-1.

### Luciferase reporter assay

The following plasmids were constructed by GenePharma (Shanghai, China): wild-type HIF-1 $\alpha$  and mutant (N803A) HIF-1 $\alpha$  in the pcDNA3 vector, HIF-1 $\alpha$  and HIF-1 $\alpha$  C-TAD knockout (KO) in the pSD11 vector, and the pGL3-HRE-KLF5-Luc luciferase reporter plasmid. HIF-1 $\alpha$  TAD-Gal4, HIF-1 $\alpha$  N-TAD-Gal4, and HIF-1 $\alpha$  C-TAD-Gal4 were constructed by inserting the sequence from Addgene plasmid #18955 into the backbone of Addgene plasmid #24887 as described previously [23]. The respective plasmids were transfected into cells using Lipofectamine 2000 according to the manufacturer's instructions (Invitrogen Corp., Carlsbad, CA, USA). Detailed methods for the luciferase reporter assay are provided in the Supplementary Methods.

### Chromatin immunoprecipitation assay

Chromatin immunoprecipitation (ChIP) was performed with a Simple ChIP Enzymatic ChIP Kit (magnetic beads) (#9003; Cell Signaling Technology, Danvers, MA, USA). Immunoprecipitation was performed with an antibody against HIF-1 $\alpha$  (ab2185; Abcam) or normal IgG as a control. Precipitated DNA fragments were detected by PCR using the following primers specific for the

promoter region of KLF5: forward 5'-CGGGCTCAAGTGATTCTCTCT-3', reverse 5'-GGAAACCCTGTCCCTACTAAAAGTA-3'.

#### Western blotting

Western blotting was performed as previously described [24]. The primary antibodies used were anti-GAPDH (CW0100M, CWBio, Beijing, China), anti-FIH-1 (NB100-428; Novus, Centennial, CO, USA), anti-HIF-1 $\alpha$  (ab2185), anti- $\alpha$ -SMA (ab5694), anti-collagen-1 (ab34710), anti-fibronectin (ab2413), anti-KLF5 (ab137676), anti-TGF- $\beta$ 1 (ab82486) and anti-Lamin B1 (ab16048) (all from Abcam, Cambridge, MA, USA). The secondary HRP-conjugated antibodies used were anti-mouse IgG and anti-rabbit IgG (Abcam).

#### Immunofluorescence and immunohistochemistry

Immunofluorescence and immunohistochemistry were performed using established methods [25]. The following primary antibodies were used: anti-HIF-1 $\alpha$  (ab2185), anti- $\alpha$ -SMA (ab5694), anti-collagen-1 (ab34710), anti-KLF5 (sc-398470; Santa Cruz Biotechnology, Dallas, TX, USA) and anti-FIH-1 (NB100-428; Novus, Centennial, CO, USA). Images were obtained by laser scanning confocal microscopy (FV-1000, Olympus, Tokyo, Japan).

#### Quantitative real-time PCR assay

Total RNA was extracted from the renal cortex and cells using RNAiso Plus reagent (total RNA extraction reagent; Takara, Shiga, Japan), and the mRNA was quantified using qRT-PCR with SYBR Green (Takara) as previously described [24]. RT-PCR was performed using an ABI PRISM 7300 Real-Time PCR System (Applied Biosystems, Foster City, USA). The relative mRNA expression was normalized to  $\beta$ -actin. All the primers for qRT-PCR are listed in Supplementary Table S1.

#### Statistical analyses

SPSS version 20.0 (IBM Corp., Armonk, NY, USA) was used for statistical analysis. Data are shown as the mean  $\pm$  SEM. For experiments comparing two groups, the *t* test or Mann-Whitney *U* test was used. When >2 groups were compared, 1-way analysis of variance followed by Dunnett's test or Bonferroni correction was employed to analyze the differences. A 2-sided *P* value < 0.05 was considered significant.

## RESULTS

### HIF-1 $\alpha$ activation is associated with the progression of CKD after AKI

Moderate and severe I/R models were established to explore the correlation of HIF-1 $\alpha$  activation with the outcome of AKI. We observed that the levels of serum creatinine (Scr) were similar to the baseline on day 14 in mice with moderate I/R; in contrast, Scr levels were significantly increased in mice with severe I/R (Fig. 1a), suggesting the progression of CKD following severe AKI. Consistent with this result, as shown in Fig. 1b and c, kidney injury had recovered on day 14 after moderate I/R, whereas morphologic lesions in the kidneys were evident on day 14 after severe I/R. Furthermore, the expression of the fibrotic markers  $\alpha$ -smooth muscle actin ( $\alpha$ -SMA), collagen-1 and fibronectin were markedly increased in kidneys with severe I/R (Fig. 1d, e). Similar results were observed in kidney sections immunostained with antibodies against  $\alpha$ -SMA and collagen-1 (Fig. 1f).

Next, HIF-1 $\alpha$  expression was assessed in kidneys with I/R. As shown by Western blotting in Fig. 1g, compared with moderate I/R, severe ischemia exhibited increased induction of HIF-1 $\alpha$  expression on day 14. This was also confirmed by immunostaining (Fig. 1h). Collectively, these results indicate that the severity of hypoxia/ischemia-induced injury is a key determinant dictating the divergent outcomes of AKI. More importantly, the progression of CKD after AKI might be associated with the activation of HIF-1 $\alpha$ .

Sustained activation of HIF-1 $\alpha$  is observed in severe AKI

We next investigated the dynamic changes in kidney injury and HIF-1 $\alpha$  expression in moderate and severe AKI after I/R. We found that the Scr level was significantly elevated on day 1 after moderate I/R but had almost returned to baseline on day 14. However, elevated Scr was observed on day 1 as well as day 14 in mice with severe I/R (Fig. 2a). Histologically, as shown in Fig. 2b, tubule injury and protein casting were observed on day 1 in mice with moderate I/R and had recovered on day 14, suggesting transient AKI followed by recovery. However, extensive tubule injury and severe protein casting occurred on day 1 in mice with severe I/R and persisted on day 14 (Fig. 2c), suggesting the progression of kidney injury.

Then, we explored the dynamics of HIF-1 $\alpha$  expression in AKI. A transient induction of HIF-1 $\alpha$  that returned to baseline levels was observed between day 1 and day 14 in mice with moderate I/R (Fig. 2d). In contrast, HIF-1 $\alpha$  was markedly induced on day 1 after the 40 min I/R treatment and was continuously expressed until day 14 (Fig. 2e). A similar expression pattern was shown by immunohistochemistry (Fig. 2f, g). Taken together, these data demonstrate that, in contrast to moderate AKI after I/R, which is characterized by transient kidney injury and recovery, CKD transition following AKI was associated with sustained activation of HIF-1 $\alpha$ .

### Inhibition of HIF-1 $\alpha$ ameliorates the progression of kidney injury following AKI

We then investigated the potential contributions of sustained activation of HIF-1 $\alpha$  to AKI-CKD progression using PX-478, a specific small molecule inhibitor of HIF-1 $\alpha$  expression and function (HIF-1-mediated gene transcription) [20]. PX-478 was administered daily by intraperitoneal injection starting on day 5 after the 40 min I/R treatment (Fig. 3a). Strikingly, we found that the Scr level on day 14 after I/R was significantly decreased in the mice that received the PX-478 treatment (Fig. 3b). Similarly, PAS and Masson staining also demonstrated ameliorated kidney injury and fibrotic lesions (Fig. 3c, d). Moreover, PX-478 reduced the mRNA and protein expression of  $\alpha$ -SMA, collagen-1, and fibronectin in renal cortical tissues, as demonstrated by Western blotting (Fig. 3e, f). Furthermore, as presented in Fig. 3g, the results were also confirmed by immunostaining with antibodies against  $\alpha$ -SMA and collagen-1. Therefore, these data indicate that blocking HIF-1 $\alpha$  activation efficiently protected the kidney against CKD progression after severe AKI.

### KLF5 is upregulated by HIF-1 $\alpha$ and promotes AKI to CKD progression

A previous study indicated that the transcriptional response to hypoxia was fine-tuned by HIF activity [26]. By using RNA-seq, we recently found that KLF5, a HIF-1 $\alpha$  transcriptional target gene, was precisely regulated according to the degree of HIF-1 $\alpha$  activation during the progression of renal fibrosis [27]. To elucidate the exact mechanism of HIF-1 $\alpha$  activities in the different outcomes of AKI, we investigated whether KLF5 plays a critical role in determining the outcome of AKI. We found that KLF5 mRNA and protein expression were significantly increased on day 14 in the kidneys of mice with severe I/R compared to those of mice with moderate I/R (Fig. 4a, b). Immunofluorescence analyses further showed that KLF5 was mainly expressed in the tubules of mice with severe I/R (Fig. 4c). Moreover, HIF-1 $\alpha$  could bind to the KLF5 promoter (Supplementary Fig. S1), demonstrating that KLF5 could be transcriptionally regulated by HIF-1 $\alpha$  under severe AKI conditions. Moreover, we found that transforming growth factor- $\beta$  (TGF- $\beta$ 1), a specific target of KLF5 signaling [27], was markedly induced (Fig. 4d). Strikingly, KLF5 expression was abrogated in the kidney after PX-478 treatment (Fig. 4e-g). Therefore, these data all indicate that KLF5 expression was stimulated by HIF-1 in severe AKI.

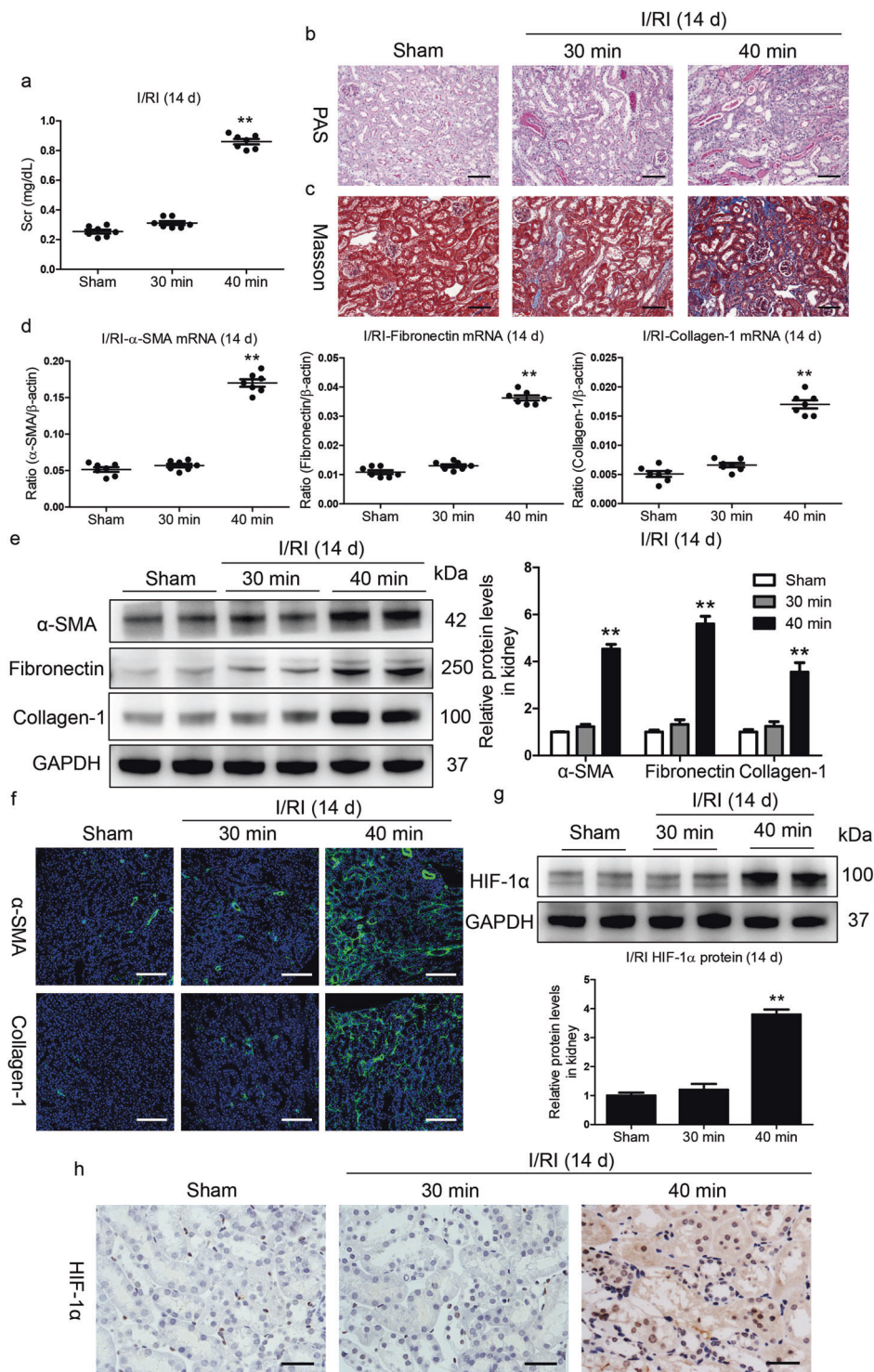


**Fig. 1** HIF-1 $\alpha$  activation is associated with poor AKI outcomes. **a** Serum creatinine (Scr) levels on day 14 after 30 or 40 min ischemia/reperfusion-induced renal injury (I/R). **b** Representative histological changes (periodic acid-Schiff [PAS] staining) on day 14 after 30 or 40 min of I/R ( $n = 7$ ). Scale bar, 100  $\mu$ m. **c** Representative images of Masson staining ( $n = 7$ ). Scale bars, 100  $\mu$ m. **d, e** Quantitative real-time polymerase chain reaction (qRT-PCR) and Western blotting analyses of  $\alpha$ -SMA, collagen-1, and fibronectin expression. The relative levels were normalized to  $\beta$ -actin or GAPDH ( $n = 7$ ). **f** Representative images of  $\alpha$ -SMA and collagen-1 immunostaining on day 14 in kidneys from mice subjected to 30 or 40 min I/R ( $n = 7$ ). Scale bar, 100  $\mu$ m. **g** Western blotting analyses of HIF-1 $\alpha$  expression in kidney tissues ( $n = 7$ ). **h** Representative images of HIF-1 $\alpha$  expression in kidney tissues from mice after 30 or 40 min of I/R. Scale bar, 50  $\mu$ m. Data are shown as the mean  $\pm$  SEM of 7 mice. \*\* $P < 0.01$  versus the sham control (Dunnett's test). GAPDH, glyceraldehyde-3-phosphate dehydrogenase.

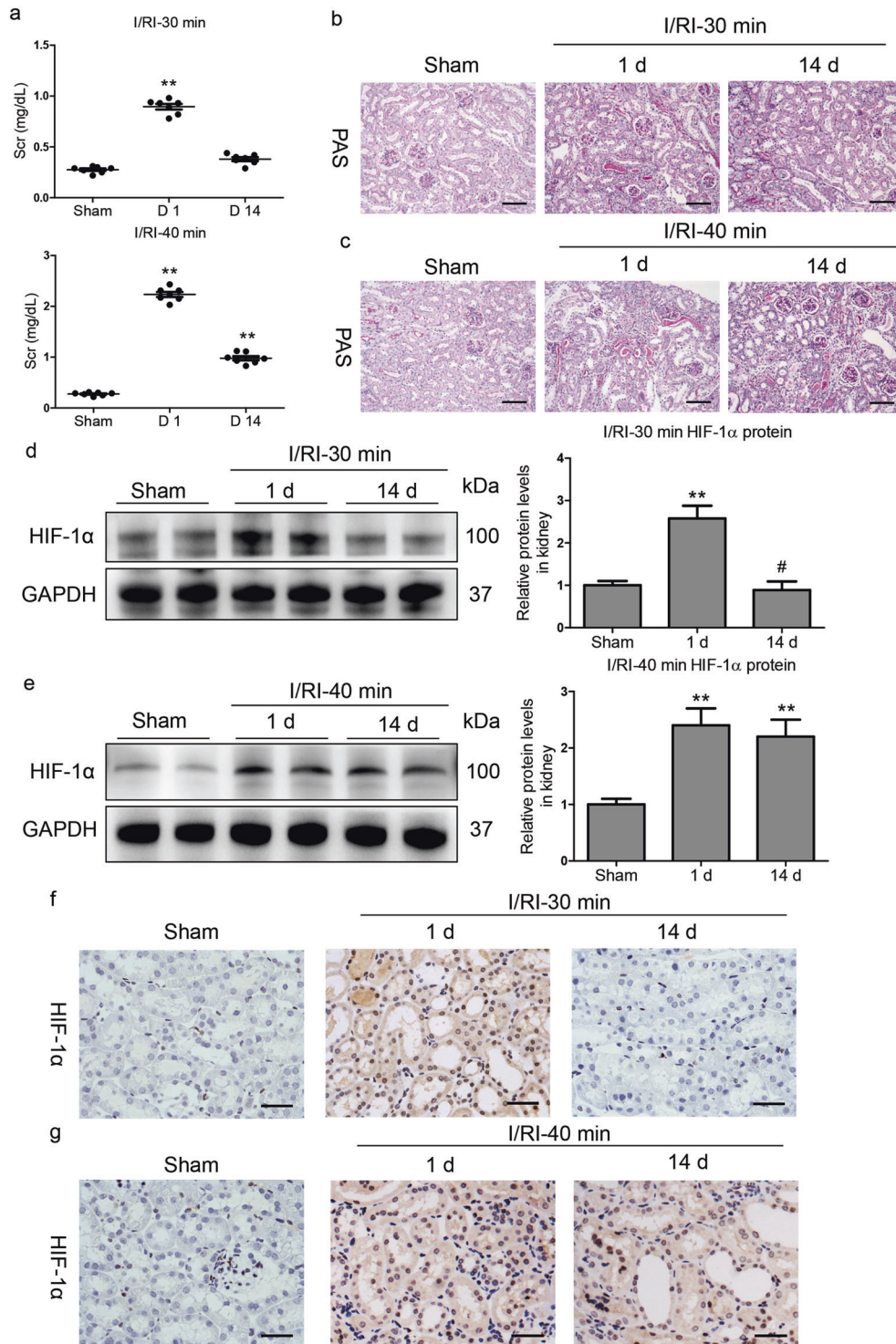


**Fig. 2 Sustained activation of HIF-1 $\alpha$  is observed in severe AKI without recovery.** **a** Scr levels were assayed at the indicated time points after 30 or 40 min of I/RI. **b, c** Representative histological changes (PAS staining) at the indicated time points after 30 or 40 min of I/RI ( $n = 7$ ). Scale bar, 100  $\mu$ m. **d, e** Western blots of HIF-1 $\alpha$  protein expression in kidney cortex tissues ( $n = 7$ ). **f, g** Representative images of HIF-1 $\alpha$  immunostaining in kidneys from mice after 30 or 40 min of I/RI. Scale bars, 50  $\mu$ m. Data are presented as the mean  $\pm$  SEM of 7 mice. D1, day 1; D14, day 14. **\*\*** $P < 0.01$  versus the sham control (Dunnett's test); **#** $P < 0.05$  versus D1 (Bonferroni correction, 2 comparisons were made).

The role of KLF5 was then further explored by an in vitro study. As shown in Fig. 4h, mouse primary TECs and HK-2 cells were treated to simulate in vivo conditions. We found that modeling moderate I/RI stimulated a low degree of HIF-1 $\alpha$  expression, whereas modeling severe I/RI stimulated a high degree of HIF-1 $\alpha$  expression (Supplementary Fig. S2a–d). Severe I/RI with a high degree of HIF-

1 $\alpha$  expression was sufficient to induce fibrogenesis of TECs and HK-2 cells, as assessed by  $\alpha$ -SMA and collagen-1 expression (Supplementary Fig. S2e–h). Furthermore, KLF5 protein expression was significantly increased in TECs with simulated severe I/RI (Supplementary Fig. S3a, b). To further characterize the possible functional effect of KLF5 on fibrogenesis in TECs, we knocked down KLF5 using

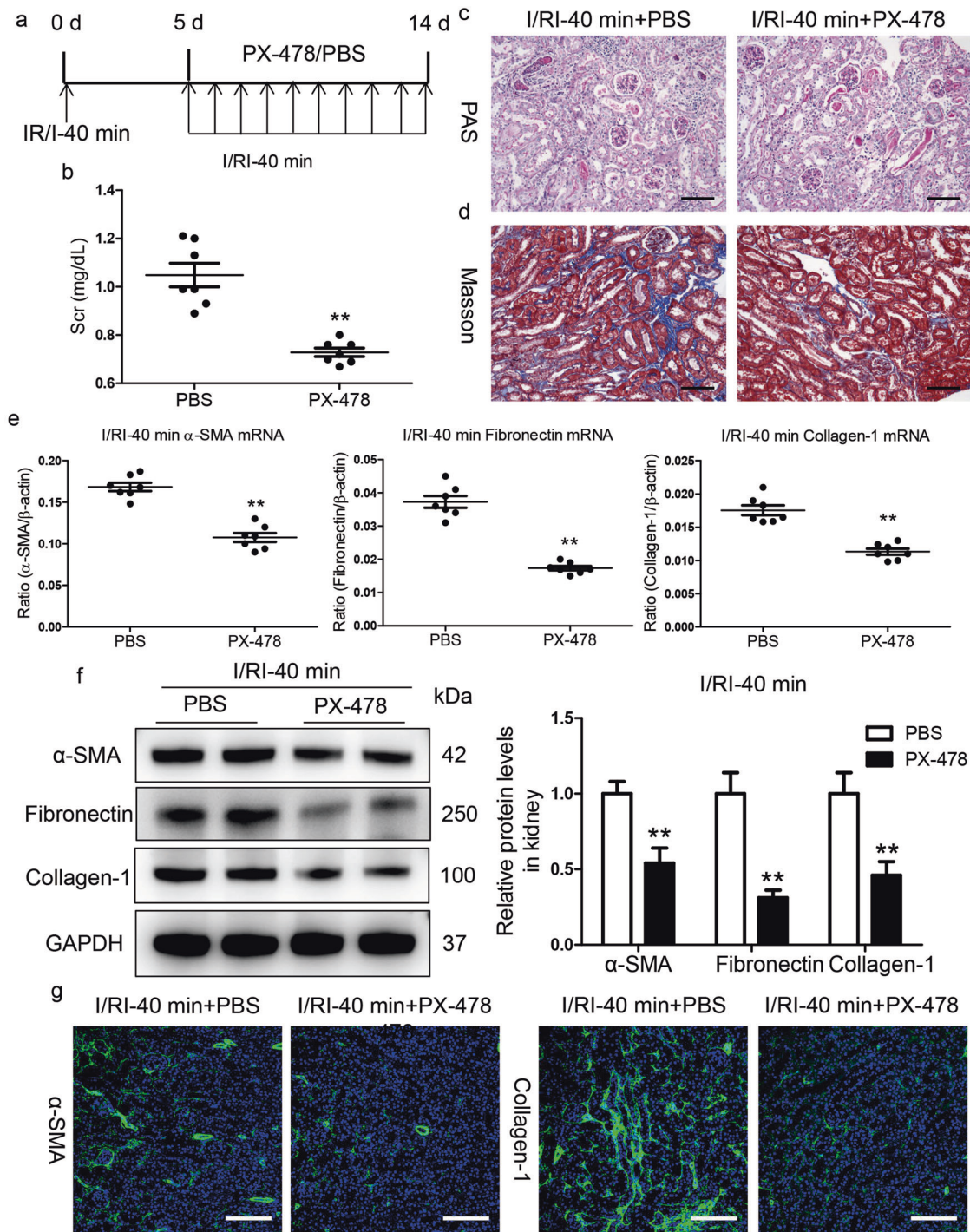


**Fig. 3** Inhibition of HIF-1 $\alpha$  by PX-478 hinders AKI to CKD progression. **a** Diagram of the experimental design. The arrows indicate the time at which PX-478 or vehicle was administered. **b** PX-478 reduced Scr levels on day 14 after I/RI. **c, d** Representative histological changes (PAS and Masson staining) after PX-478 treatment in mice subjected to 40 min of I/RI ( $n = 7$ ). Scale bar, 100  $\mu$ m. **e** Inhibition of HIF-1 $\alpha$  by PX-478 abolished the mRNA expression of  $\alpha$ -SMA, collagen-1, and fibronectin in the kidneys of mice after 40 min of I/RI ( $n = 7$ ). **f** PX-478 treatment reduced the protein expression of fibronectin, collagen-1, and  $\alpha$ -SMA in the kidneys of mice after 40 min of I/RI ( $n = 7$ ). The quantified expression levels are shown in the right panel. **g** Representative micrographs showing changes in  $\alpha$ -SMA and collagen-1 immunostaining on day 14 after PX-478 treatment. Scale bars, 100  $\mu$ m. Data are presented as the mean  $\pm$  SEM of seven mice. **\*\*** $P < 0.01$  versus the PBS control (Mann–Whitney  $U$  test).

siRNA and demonstrated that it markedly diminished the expression of TGF- $\beta$ 1, a specific target of KLF5 signaling (Fig. 4i). Moreover,  $\alpha$ -SMA expression was also reduced significantly (Fig. 4j, k). This was further checked by in vivo experiments. We found that KLF5-targeted siRNA (siKLF5) significantly reduced Scr levels (Fig. 4l) and

attenuated fibrotic lesions (Fig. 4m). Consistent with these results, siKLF5 significantly abrogated the expression of  $\alpha$ -SMA and collagen-1 (Supplementary Fig. S4). Together, these results demonstrate that abnormal activation of HIF-1 $\alpha$  promoted CKD progression following AKI via activating KLF5 signaling.

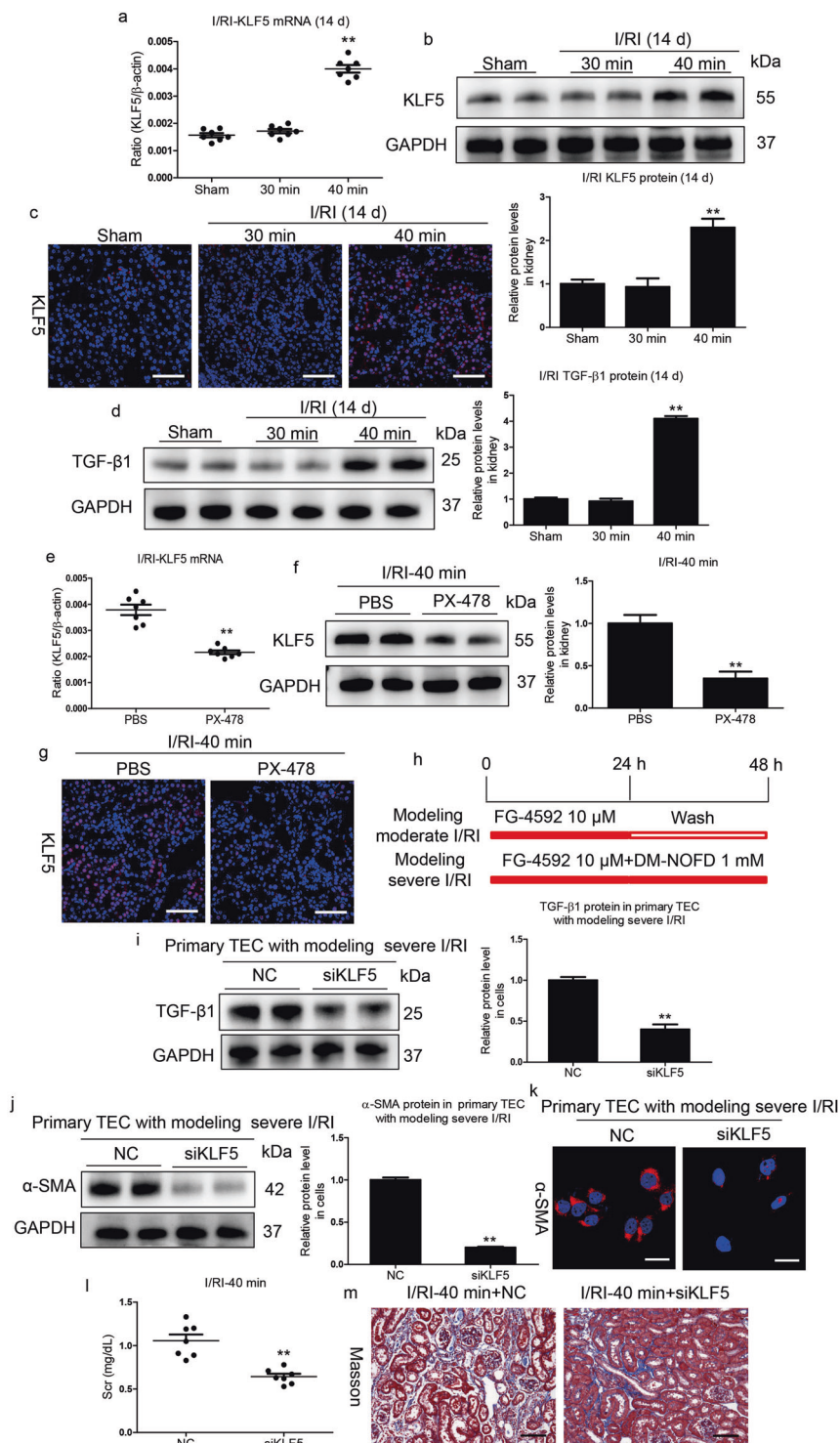


**Fig. 4** KLF5 promotes progression of CKD following AKI. **a** Relative mRNA levels of KLF5 in different groups. **b** Kidney cortex tissues were immunoblotted with specific antibodies against KLF5 and GAPDH ( $n = 7$ ).  $**P < 0.01$  versus the sham control (Dunnett's test). **c** Representative images of KLF5 immunostaining on day 14 in kidneys from mice subjected to 30 or 40 min I/RI ( $n = 7$ ). Scale bars, 50  $\mu\text{m}$ . **d** Western blotting analyses of TGF- $\beta$ 1 expression. The relative levels were normalized to GAPDH ( $n = 7$ ). **e**, **f** PX-478 reduced the mRNA and protein levels of KLF5 on day 14 in mice subjected to 40 min of I/RI ( $n = 7$ ). **g** Representative micrographs showing changes in KLF5 on day 14 after PX-478 treatment. Scale bars, 50  $\mu\text{m}$ . Data are presented as the mean  $\pm$  SEM of seven mice.  $**P < 0.01$  versus the PBS control (Mann-Whitney  $U$  test). **h** Diagram of the experimental design. Moderate I/RI was simulated in the indicated cells by treatment with FG-4592 (10  $\mu\text{M}$ ) for 24 h, washing, and incubation without FG-4592 for an additional 24 h. Severe I/RI was simulated in cells by incubation with FG-4592 (10  $\mu\text{M}$ ) and DM-NOFD (1 mM) continuously for 48 h. **i** KLF5 was knocked down with siRNA in primary TECs with simulated severe I/RI, and TGF- $\beta$ 1 levels were analyzed by Western blotting ( $n = 3$ ). **j**, **k** KLF5 was knocked down with siRNA in primary TECs with simulated severe I/RI, and  $\alpha$ -SMA levels were analyzed by Western blotting and immunofluorescence ( $n = 3$ ). Scale bars, 20  $\mu\text{m}$ . **l** Scr levels in mice subjected to 40 min of I/RI following KLF5 knockdown. **m** Representative images of Masson staining after KLF5 siRNA administration. Scale bars, 100  $\mu\text{m}$ . Data are presented as the mean  $\pm$  SEM for groups of seven mice.  $**P < 0.01$  versus the scrambled negative control group (Mann-Whitney  $U$  test).

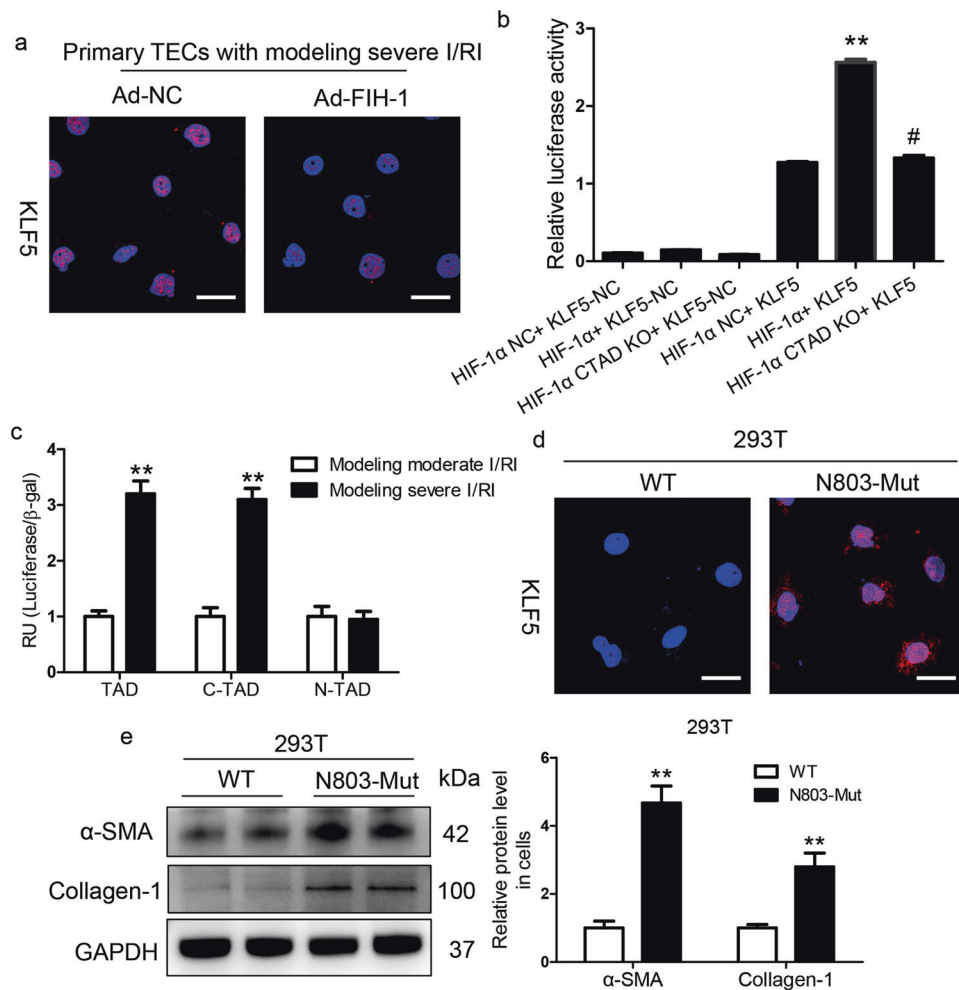


**Fig. 5** KLF5 was transcriptionally regulated by the HIF-1α C-TAD. **a** KLF5 expression was analyzed in primary TECs with simulated severe I/RI after FIH-1 was overexpressed with adenovirus (Ad-FIH-1). Scale bars, 20 μm. **b** Luciferase reporter assays were performed using constructs with HIF-1α or HIF-1α C-TAD KO. 293T cells were transfected with these constructs along with the HRE-KLF5-Luc overexpression plasmid. Data were obtained from four independent experiments. \*\**P* < 0.01 versus the HIF-1α-NC (pcDNA3 empty vector) + HRE-KLF5-Luc group; #*P* < 0.01 versus the HIF-1α+KLF5-Luc group (Bonferroni correction, two comparisons were made). **c** The HIF-1α N-TAD+ C-TAD-Gal4, HIF-1α N-TAD-Gal4, or HIF-1α C-TAD-Gal4 construct was co-transfected into 293T cells with either the KLF5-Luc construct or empty vector followed by simulated moderate or severe I/RI for 24 h. The transfection efficiency was corrected by the β-galactosidase controls. Data are shown as the mean of four separate experiments ± SEM. \*\**P* < 0.01 versus cells with simulated moderate I/RI (Dunnett's test). **d** Expression of KLF5 protein determined by immunofluorescence in 293T cells transfected with HIF-1α-WT or HIF-1α-N803A-mutant for 48 h (*n* = 4). Scale bars, 100 μm. **e** The protein expression of α-SMA and collagen-1 in 293T cells transfected with HIF-1α-WT or HIF-1α-N803A-mutant for 48 h was determined by Western blotting. Data were obtained from four independent experiments. \*\**P* < 0.01, by Bonferroni post hoc test after 2-way ANOVA.

#### KLF5 is stimulated by the HIF-1α C-TAD under severe hypoxic conditions

Next, the underlying mechanism of the fibrogenesis response regulated by HIF-1α was explored. HIF-1α contains two independent transcriptional activation domains (TADs), the N-TAD and the C-TAD, among which the C-TAD is regulated by FIH-1. We found that the increased expression of KLF5 was diminished after adenovirus-FIH-1 (Ad-FIH-1) transfection in primary TECs treated with simulated severe I/RI (Fig. 5a). We then asked whether KLF5 was directly stimulated by the HIF-1α C-TAD. Based on the luciferase reporter assay, compared with the controls, HIF-1α C-TAD KO markedly reduced KLF5 activity (Fig. 5b), indicating transcriptional regulation of KLF5 by the HIF-1α C-TAD. In 293T cells, HIF-1α TAD-Gal4, which contained the entire TAD region (N-TAD and C-TAD), was activated following simulated severe I/RI. This induction was mimicked by HIF-1α C-TAD-Gal4 (C-TAD only; a.a. 776–826) but not by HIF-1α N-TAD-Gal4 (N-TAD only; a.a. 530–652) (Fig. 5c).

The function of the HIF-1α C-TAD is regulated by the action of FIH-1 on residue N803 within the C-TAD of HIF-1α. We assessed the hypothesis that the transcriptional effect of HIF-1α on KLF5 was regulated by asparaginyl hydroxylation at residue N803. Therefore, a single mutant HIF-1α at residue N803 (N803-Mut) and wild-type HIF-1α (WT) were constructed (Supplementary Fig. S5) and analyzed. We found that KLF5 expression was significantly induced in cells transfected with the N803-Mut plasmid compared to the WT plasmid-transfected cells (Fig. 5d). Furthermore, a fibrotic phenotype was also induced in the N803-Mut-transfected cells, as evidenced by the protein levels of α-SMA and collagen-1 (Fig. 5e). These results indicate that KLF5 was transcriptionally stimulated by the HIF-1α C-TAD under severe hypoxic conditions.

#### HIF-1α C-TAD activation augments AKI to CKD transition

To clarify the role of the HIF-1α C-TAD in the AKI to CKD transition in vivo, HIF-1α C-TAD overexpression in mice with 30 min I/RI was performed by Lv-HIF-1α C-TAD injection through the tail vein.



Overexpression of the HIF-1 $\alpha$  C-TAD significantly promoted the progression of ischemia/hypoxia-induced kidney injury in Lv-HIF-1 $\alpha$  C-TAD-injected mice compared to that in Lv-NC-injected mice, as evidenced by Scr levels and PAS and Masson staining (Fig. 6a–c). Indeed, Lv-HIF-1 $\alpha$  C-TAD administration markedly promoted the transcript (Fig. 6d) and protein (Fig. 6e) levels of  $\alpha$ -SMA and collagen-1 in the kidneys of mice subjected to 30 min of I/RI. These findings were also confirmed by immunofluorescence analyses (Fig. 6f). In addition, we found that the overexpression of the HIF-1 $\alpha$  C-TAD markedly increased the transcript (Fig. 6g) and protein (Fig. 6h) levels of KLF5 in mice with AKI. As expected, the levels of TGF- $\beta$ 1, the specific target of KLF5 signaling, also increased significantly (Fig. 6i). Thus, HIF-1 $\alpha$  C-TAD activation contributes to the AKI to CKD transition via KLF5 stimulation.

FIH-1 is the key factor influencing the outcome of AKI

Next, we investigated the potential mechanism underlying the regulation of specific HIF target genes under varied AKI severities. HIF-1 could be regulated by PHD and FIH-1. PHD activity is supposedly more sensitive to hypoxia than that of FIH-1 [28]. Therefore, we speculated that FIH-1 was the critical factor determining the precise regulation of HIF-1 transcriptional responses in ischemia/hypoxia-induced AKI. To this end, we examined the expression of FIH-1 in the kidneys of mice with moderate and severe AKI. We found that FIH-1 expression was not altered in whole renal cortical lysates of mice with moderate I/RI, whereas it significantly decreased in mice with severe I/RI (Fig. 7a). Given that HIF-1 $\alpha$  enters the nuclei during ischemia/hypoxia-induced AKI, we expected FIH-1 in the nuclei to regulate HIF-1 activity. Therefore, the expression of FIH-1 in nuclear lysates of renal cortical tissue was examined. Remarkably, we found that the expression of FIH-1 was markedly decreased in the nuclear lysates of mice after 40 min of I/RI (Fig. 7b), suggesting that the transcriptional response of HIF-1 $\alpha$ , which is negatively regulated by FIH-1, was not repressed. Furthermore, FIH-1 expression was also examined by immunofluorescence analyses. As shown in Fig. 7c, in the normal kidney, FIH-1 was mainly localized in the cytoplasm. However, in the kidneys of mice with severe I/RI, FIH-1 expression was decreased in both the nuclei and cytoplasm on day 14.

The function of FIH-1 was also explored *in vitro*. We found that FIH-1 expression was significantly decreased in whole lysates of primary TECs with simulated severe I/RI, as detected by Western blotting (Fig. 7d). As expected, nuclear FIH-1 expression was significantly increased in primary TECs with simulated moderate I/RI (Fig. 7e). The results were also confirmed in HK-2 cells (Fig. 7f). To further characterize the key functional role of FIH-1 in suppressing fibrogenesis of TECs, FIH-1 was overexpressed with Ad-FIH-1. We observed a marked reduction in  $\alpha$ -SMA and collagen-1 levels (Fig. 7g), indicating the inhibition of fibrogenesis of TECs. Furthermore, to investigate whether FIH-1 directly interacts with HIF-1 $\alpha$  in tubules, we immunoprecipitated proteins isolated from primary TECs using the HIF-1 $\alpha$  antibody followed by blotting with a FIH-1 antibody and revealed that the amount of FIH-1 directly bound to HIF-1 $\alpha$  in primary TECs with simulated moderate I/RI was significantly higher than that in cells with simulated severe I/RI (Fig. 7h). Similar results were observed in HK-2 cells (Fig. 7i). Thus, the results suggest that FIH-1 is the key factor determining the outcomes of AKI.

FIH-1 overexpression prevents AKI to CKD progression

To confirm the functional effects of FIH-1 on AKI to CKD progression *in vivo*, FIH-1 was overexpressed in mice with severe I/RI using Lv-FIH-1 injection via the tail vein. The efficiency of overexpression in tubules from the renal cortex was evaluated (Supplementary Fig. S6). Compared with the control mice, the mice overexpressing FIH-1 showed efficient abrogation of the elevated Scr levels (Fig. 8a). Importantly, tubule injury and protein casting were significantly

diminished in the kidneys of Lv-FIH-1-injected mice with severe AKI (Fig. 8b), suggesting that FIH-1 has a protective role in halting the progression of AKI to CKD. Indeed, Lv-FIH-1-driven abrogation of kidney disease progression was evidenced by Masson staining (Fig. 8c), the transcript (Fig. 8d) and protein (Fig. 8e) levels of  $\alpha$ -SMA and collagen-1, and immunofluorescence analyses (Fig. 8f). In addition, we also found that the overexpression of FIH-1 significantly reversed the increase in KLF5 (Fig. 8g, h). Thus, the overexpression of FIH-1 dramatically abrogated the progression of kidney disease following AKI, implying that FIH-1 has a protective effect against the AKI to CKD transition.

## DISCUSSION

Convincing studies have shown that a single episode of AKI can lead to subsequent progressive and fibrotic CKD [1, 2, 29]. However, the role of HIF-1 $\alpha$  in AKI to CKD progression is poorly understood. In the present study, we investigated the molecular mechanisms that govern HIF-1 $\alpha$  involvement in the distinct fates of the kidneys after AKI. We clearly demonstrated that tubular HIF-1 $\alpha$  C-TAD, which was activated in severe AKI due to the loss of FIH-1, played a critical role in driving AKI to CKD progression via transcriptional regulation of KLF5. However, during mild/moderate ischemic injury, the transcriptional response of the HIF-1 $\alpha$  C-TAD was inhibited due to functional FIH-1 in tubules, resulting in the recovery of kidney function. Collectively, these findings elucidate the molecular mechanism by which HIF-1 activity affects the AKI to CKD transition and provide a therapeutic strategy for halting hypoxia-mediated AKI to CKD progression.

Hypoxia is a critical instigator in the progression from AKI to CKD. However, the exact mechanism underlying the hypoxia-dependent progression of kidney diseases has not been clarified. HIF is a critical transcription factor regulating the hypoxia response and the master transcriptional regulator of hypoxia. Recently, Shu and Dong et al. [30] summarized that tubular HIF-1 $\alpha$  has pleiotropic effects on kidney injury and repair. Our previous research also revealed degree-dependent biphasic effects of HIF-1 $\alpha$  on CKD progression. Namely, moderate activation of HIF-1 $\alpha$  prevents CKD, while paradoxically, excessive activation of HIF-1 $\alpha$  promotes the progression of CKD [27]. This finding encouraged us to further explore the possible role of tubular HIF-1 $\alpha$  in mediating CKD following hypoxia-induced AKI. In this study, in contrast to transient activation of HIF-1 $\alpha$  in kidneys with mild/moderate I/RI, sustained activation of HIF-1 was found in kidneys with severe I/RI. Indeed, our data revealed that the degree of HIF activation was the main regulator of the outcome of AKI. Thus, we speculate that excessive and sustained activation of HIF-1 might contribute to the AKI to CKD transition.

Previous studies showed that HIF-1 protein was activated by graded hypoxia in a degree-dependent manner [31]. Furthermore, the number of modulated target genes was associated with the degree of HIF-1 activation [32], suggesting that the regulation of HIF-related gene expression may vary with hypoxia severity. Our previous data demonstrated differences in transcriptome features observed under conditions of moderate or excessive HIF-1 activation. Importantly, KLF5, which is transcriptionally regulated by HIF-1 $\alpha$ , plays a crucial role in renal fibrosis [27]. Interestingly, in the present study, we found that tubular KLF5 was only induced by HIF-1 in severe AKI and was required for fibrogenesis of TECs. Moreover, we demonstrated the pathological effects of KLF5 in subsequent progressive and fibrotic CKD after AKI *in vivo*. Chen et al. [33] demonstrated that KLF5 was expressed in tubular cells and associated with the pathogenesis of renal fibrosis in fibrotic kidneys. KLF5 is reportedly a critical determinant in the remodeling of injured tissue through the production of extracellular matrix proteins and a variety of paracrine factors [34]. Thus, KLF5 activation induced by HIF-1 represents a novel mechanism for the progression of severe AKI to fibrotic CKD.

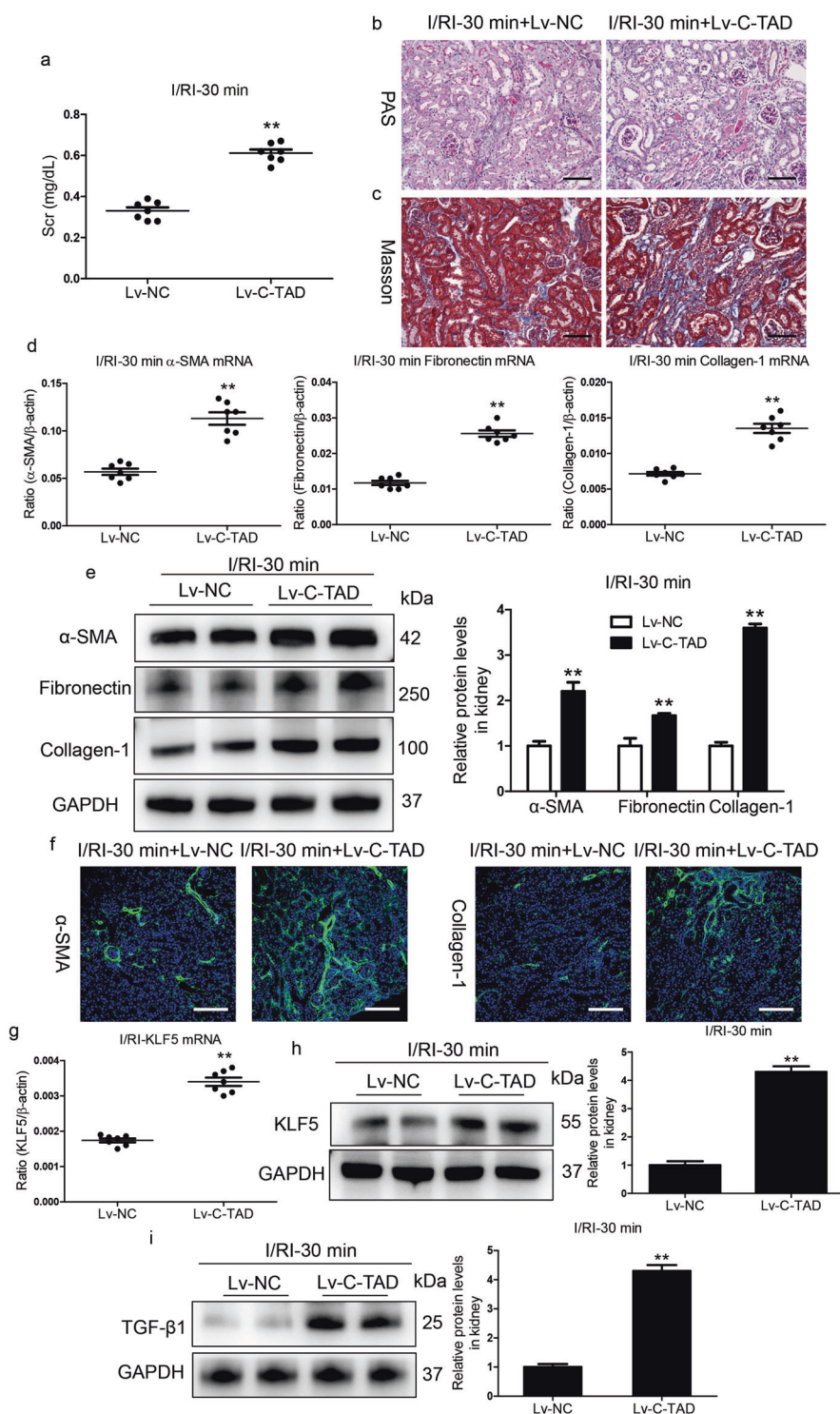


**Fig. 6** Activation of the HIF-1 $\alpha$  C-TAD promotes AKI to CKD progression. **a** Scr levels in mice subjected to 30 min of I/RI following Lv-HIF-1 C-TAD administration. **b, c** Representative images of PAS or Masson staining on day 14 of the kidneys of mice subjected to 30 min of I/RI following Lv-HIF-1 C-TAD injection ( $n = 7$ ). Scale bars, 100  $\mu$ m. **d** qRT-PCR analyses of  $\alpha$ -SMA, collagen-1, and fibronectin mRNA expression on day 14 in kidney tissues from mice injected with Lv-HIF-1 C-TAD ( $n = 7$ ). **e** The protein expression of  $\alpha$ -SMA, collagen-1, and fibronectin in the kidney cortex of mice subjected to 30 min of I/RI following Lv-HIF-1 C-TAD administration was assessed by Western blotting analyses ( $n = 7$ ). **f** Representative images of  $\alpha$ -SMA and collagen-1 immunostaining in kidney tissues from mice subjected to 30 min of I/RI following Lv-HIF-1 C-TAD injection ( $n = 7$ ). Scale bars, 100  $\mu$ m. **g, h** qRT-PCR and Western blotting analyses of KLF5 expression in the indicated groups. **i** Western blotting analyses of TGF- $\beta$ 1 expression in the indicated groups. \*\* $P < 0.01$  versus Lv-NC. Data are presented as the mean  $\pm$  SEM of 7 mice. Lv-NC served as the control. \*\* $P < 0.01$  versus Lv-NC (Mann-Whitney  $U$  test).

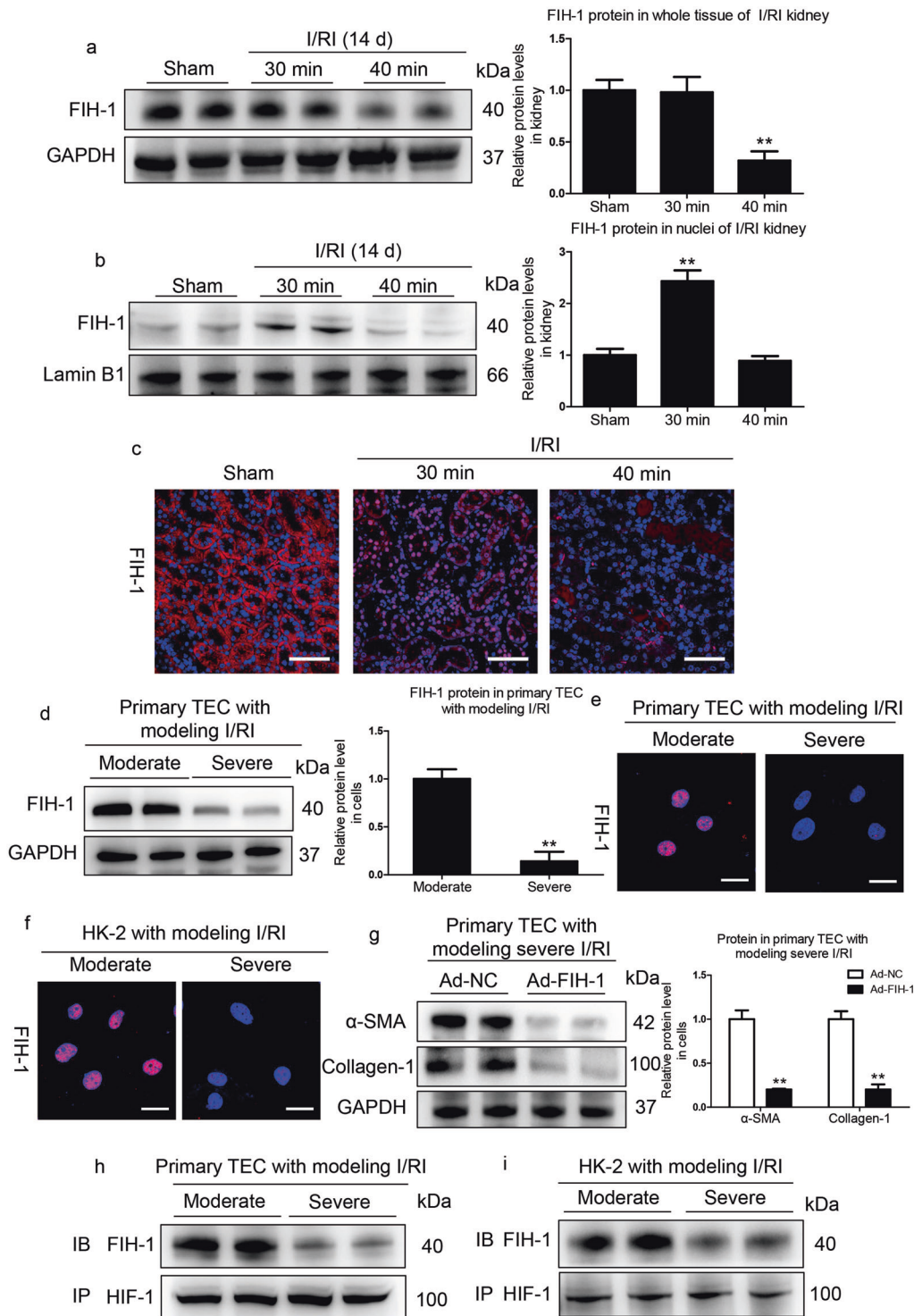


**Fig. 7 Decreased tubular FIH-1 mediates the AKI to CKD transition.** **a** Western blotting analyses of the total protein levels of FIH-1 on day 14 in kidneys of mice subjected to 30 or 40 min of I/RI ( $n = 7$ ). **b** Western blotting analyses showing nuclear levels of FIH-1. The quantified expression levels are shown in the right panel ( $n = 7$ ). The relative expression was normalized to Lamin B1. **c** Representative results of FIH-1 immunostaining. Scale bars, 50  $\mu$ m. Data are presented as the mean  $\pm$  SEM of seven mice. **\*\*** $P < 0.01$  versus the sham control (Dunnett's test). D1, day 1; D14, day 14. **d** Western blotting analyses of FIH-1 expression in primary TECs after simulated moderate or severe I/RI. Data were obtained from three independent experiments. **\*\*** $P < 0.01$  compared with cells exposed to simulated moderate I/RI. **e** Immunofluorescence staining showing FIH-1 expression in primary TECs with different treatments ( $n = 4$ ). Scale bars, 20  $\mu$ m. **f** Immunofluorescence staining showing FIH-1 expression in HK-2 cells with different treatments ( $n = 4$ ). Scale bars, 20  $\mu$ m. **g** FIH-1 was overexpressed using adenovirus (Ad-FIH-1) in primary TECs after simulated severe I/RI. The quantified expression levels are shown in the right panel ( $n = 3$ ). **\*\*** $P < 0.01$  compared with cells exposed to Ad-NC (control). **h, i** Immunoprecipitation (IP) of proteins isolated from cells with an antibody against HIF-1 $\alpha$  followed by immunoblotting (IB) analyses with a FIH-1 antibody showed the interaction of HIF-1 $\alpha$  and FIH-1 in cells exposed to moderate or severe I/RI. Rabbit IgG served as the control ( $n = 4$ ).

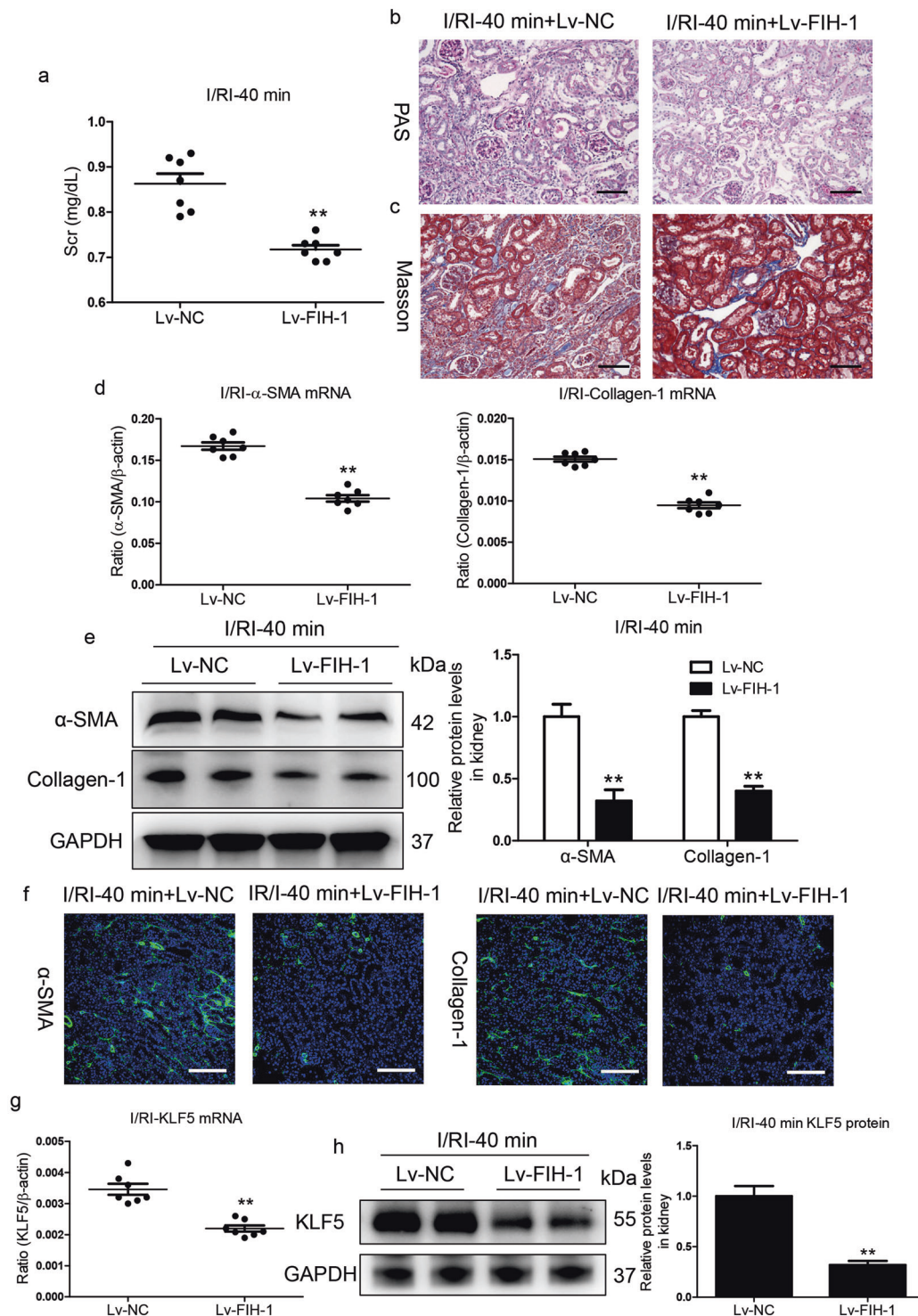


**Fig. 8** FIH-1 contributes to recovery of severe AKI. **a** Scr levels on day 14 in mice subjected to 40 min of I/RI following Lv-FIH-1 administration. **b, c** Representative images of PAS or Masson staining after Lv-FIH-1 administration ( $n = 7$ ). Scale bars, 100  $\mu$ m. **d** qRT-PCR analyses of  $\alpha$ -SMA and collagen-1 mRNA expression on day 14 in the kidneys of mice subjected to 40 min of I/RI following Lv-FIH-1 injection ( $n = 7$ ). Scale bars, 100  $\mu$ m. **e** Representative Western blot and quantitative data of renal  $\alpha$ -SMA and collagen-1 protein expression ( $n = 7$ ). Data are presented as fold induction over Lv-NC (control). **f** Representative images showing kidney sections stained with specific antibodies against  $\alpha$ -SMA and collagen-1 ( $n = 7$ ). **g, h** qRT-PCR and Western blotting analyses of KLF5 expression in the indicated groups. Scale bars, 100  $\mu$ m. Data are presented as the mean  $\pm$  SEM,  $n = 7$ . Lv-NC served as the control.  $^{***}P < 0.01$  versus Lv-NC (Mann-Whitney  $U$  test).

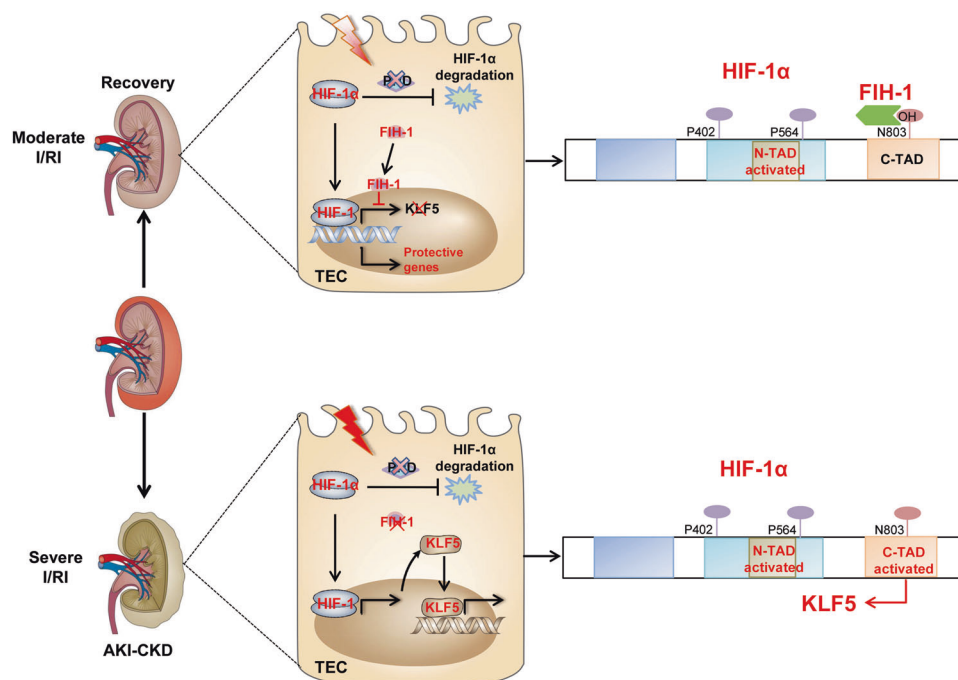


**Fig. 9 Schematic diagram showing the proposed mechanism of AKI in CKD progression.** During AKI to CKD progression, loss of tubular FIH-1 contributed to the activation of the HIF-1 $\alpha$  C-TAD, promoting the progression of CKD by transcriptionally upregulating KLF5, a HIF-1 $\alpha$  C-TAD-specific target gene.

Generally, the HIF system works to enable cells to adapt to limited oxygen availability; however, the oxygen-dependent biphasic effects of HIF-1 activation on the progression of CKD following AKI are of particular interest. Preclinical studies have indicated that HIF activation could have some harmful effects, including fibrogenesis [15–17, 35, 36], although the precise regulatory pathways for these effects are unclear. HIF-1 $\alpha$  possesses two TADs, namely, N-TAD and C-TAD. HIF-1 stabilization (N-TAD) is regulated by PHD, which catalyzes the trans-4-prolyl hydroxylation of HIF-1 at specific sites in the oxygen-dependent degradation domains. HIF-1 activity (C-TAD) is regulated by FIH-1, which catalyzes the hydroxylation of an asparaginyl residue, leading to reduced interaction between HIF-1 and transcriptional coactivators [37]. Convincing evidence has demonstrated that FIH-1 is more active at lower oxygen concentrations than PHDs, and most HIF-related genes are positively sensitive to FIH-1 silencing [26, 32], suggesting that the expression of distinct genes through the bifunctional transcriptional character of HIF-1 could be determined by FIH-1. We hypothesized that KLF5 transcriptional regulation by HIF-1 could be controlled by FIH-1. Indeed, in this study, a significant decrease in FIH-1 expression was observed in severe AKI, and KLF5 was transcriptionally regulated by HIF-1 due to the loss of FIH-1. Moreover, FIH-1 overexpression ameliorated fibrotic CKD progression in severe AKI via KLF5 inhibition, whereas recovery from mild/moderate AKI occurred instead of subsequent progressive and fibrotic CKD when HIF-1 C-TAD activity was overexpressed. Relevant to our findings, a study showed that activation of the C-TAD is essential for HIF-1 $\alpha$ -mediated angiogenic effects through transcriptional expression of the VEGF gene [38]. Yeh et al. [39] noted that FIH-1-dependent HIF-1 C-TAD target genes were not induced upon PHD inhibitor treatment but only upon stimulation of the function of the HIF-1 N-TAD. Thus, FIH-1 may be a critical regulator of HIF-1 $\alpha$ -induced KLF5 expression, contributing to the progression of AKI to CKD.

Specific PHD inhibitors, which only stimulate the function of the HIF-1 $\alpha$  N-TAD, have been used for treating renal anemia [40]. It is clinically important to elucidate the exact functions of the C-TAD

and N-TAD. To our knowledge, this study represents the first discussion of this concern. We demonstrated that the HIF-1 $\alpha$  C-TAD, not the N-TAD, played a critical role in CKD progression by transcriptionally stimulating KLF5. Thus, our findings highlight a previously unrecognized function of the HIF-1 $\alpha$  C-TAD and provide new insights into the pleiotropic effects of HIF-1 activation in AKI.

In summary, we demonstrated that loss of tubular FIH-1 contributed to the activation of HIF-1 $\alpha$  C-TAD, promoting the progression of CKD by transcriptionally upregulating KLF5, a specific HIF-1 $\alpha$  C-TAD target gene (Fig. 9). These findings provide a new understanding of the molecular mechanisms of hypoxia-induced AKI to CKD progression and indicate a novel strategy for the prevention of AKI to CKD progression.

#### ACKNOWLEDGEMENTS

The authors thank Chen-chen Zhang (Southeast University School of Medicine) for confocal image acquisition and valuable technical support. This study was supported by the National Natural Science Foundation of China (82000648, 8203000544, 81720108007, and 81470922), the National Key Research and Development Program of China (2018YFC1314002), the Natural Science Foundation of Jiangsu Province (BK20200363), the Innovative and Entrepreneurial Talent (Doctor) of Jiangsu Province and the Special Fund for Basic Scientific Research of Central Universities (2242020K40151).

#### AUTHOR CONTRIBUTIONS

ZLL, BW, and BCL designed the study, carried out experiments, analyzed data, and wrote and edited the paper; LLL, TTT, YW, STF, and JYC carried out experiments and analyzed the data; and XXZ and SDC made the figures and edited the paper; all authors approved the final version of the paper.

#### ADDITIONAL INFORMATION

**Supplementary information** The online version contains supplementary material available at <https://doi.org/10.1038/s41401-021-00617-4>.

**Competing interests:** The authors declare no competing interests.

## REFERENCES

1. See EJ, Jayasinghe K, Glassford N, Bailey M, Johnson DW, Polkinghorne KR, et al. Long-term risk of adverse outcomes after acute kidney injury: a systematic review and meta-analysis of cohort studies using consensus definitions of exposure. *Kidney Int.* 2019;95:160–72.
2. Chawla LS, Amdur RL, Amodeo S, Kimmel PL, Palant CE. The severity of acute kidney injury predicts progression to chronic kidney disease. *Kidney Int.* 2011;79:1361–9.
3. Hoste EAJ, Kellum JA, Selby NM, Zarbock A, Palevsky PM, Bagshaw SM, et al. Global epidemiology and outcomes of acute kidney injury. *Nat Rev Nephrol.* 2018;14:607–25.
4. Ferencik DA, Bonventre JV. Mechanisms of maladaptive repair after AKI leading to accelerated kidney ageing and CKD. *Nat Rev Nephrol.* 2015;11:264–76.
5. Ullah MM, Basile DP. Role of renal hypoxia in the progression from acute kidney injury to chronic kidney disease. *Semin Nephrol.* 2019;39:567–80.
6. Yang L, Besschetnova TY, Brooks CR, Shah JV, Bonventre JV. Epithelial cell cycle arrest in G2/M mediates kidney fibrosis after injury. *Nat Med.* 2010;16:535–43. 1p following 143
7. Xiao L, Zhou D, Tan RJ, Fu HH, Zhou LL, Hou FF, et al. Sustained activation of Wnt/ $\beta$ -catenin signaling drives AKI to CKD progression. *J Am Soc Nephrol.* 2016;27:1727–40.
8. Tanaka S, Tanaka T, Nangaku M. Hypoxia as a key player in the AKI-to-CKD transition. *Am J Physiol Ren Physiol.* 2014;307:F1187–95.
9. Chevalier RL. The proximal tubule is the primary target of injury and progression of kidney disease: role of the glomerulotubular junction. *Am J Physiol Ren Physiol.* 2016;311:F145–61.
10. Takaori K, Nakamura J, Yamamoto S, Nakata H, Sato Y, Takase M, et al. Severity and frequency of proximal tubule injury determines renal prognosis. *J Am Soc Nephrol.* 2016;27:2393–406.
11. Liu BC, Tang TT, Lv LL, Lan HY. Renal tubule injury: a driving force toward chronic kidney disease. *Kidney Int.* 2018;93:568–79.
12. Schödel J, Ratcliffe PJ. Mechanisms of hypoxia signalling: new implications for nephrology. *Nat Rev Nephrol.* 2019;15:641–59.
13. Hill P, Shukla D, Tran MG, Aragonés J, Cook HT, Carmeliet P, et al. Inhibition of hypoxia inducible factor hydroxylases protects against renal ischemia-reperfusion injury. *J Am Soc Nephrol.* 2008;19:39–46.
14. Bernhardt WM, Câmpean V, Kany S, Jürgensen JS, Weidemann A, Warnecke C, et al. Preconditional activation of hypoxia-inducible factors ameliorates ischemic acute renal failure. *J Am Soc Nephrol.* 2006;17:1970–8.
15. Kimura K, Iwano M, Higgins DF, Yamaguchi Y, Nakatani K, Harada K, et al. Stable expression of HIF-1 $\alpha$  in tubular epithelial cells promotes interstitial fibrosis. *Am J Physiol Ren Physiol.* 2008;295:F1023–9.
16. Higgins DF, Kimura K, Bernhardt WM, Shrimanker N, Akai Y, Hohenstein B, et al. Hypoxia promotes fibrogenesis in vivo via HIF-1 stimulation of epithelial-to-mesenchymal transition. *J Clin Invest.* 2007;117:3810–20.
17. Li ZL, Lv LL, Tang TT, Wang B, Feng Y, Zhou LT, et al. HIF-1 $\alpha$  inducing exosomal microRNA-23a expression mediates the cross-talk between tubular epithelial cells and macrophages in tubulointerstitial inflammation. *Kidney Int.* 2019;95:388–404.
18. Tang TT, Wang B, Wu M, Li ZL, Feng Y, Cao JY, et al. Extracellular vesicle-encapsulated IL-10 as novel nanotherapeutics against ischemic AKI. *Sci Adv.* 2020;6:eaa0748.
19. Luo CW, Zhou S, Zhou ZM, Liu YH, Yang L, Liu JF, et al. Wnt9a promotes renal fibrosis by accelerating cellular senescence in tubular epithelial cells. *J Am Soc Nephrol.* 2018;29:1238–56.
20. Li Z, You Q, Zhang X. Small-molecule modulators of the hypoxia-inducible factor pathway: development and therapeutic applications. *J Med Chem.* 2019;62:5725–49.
21. McDonough MA, McNeill LA, Tilliet M, Magalang UJ, Scherer PE. Selective inhibition of factor inhibiting hypoxia-inducible factor. *J Am Chem Soc.* 2005;127:7680–1.
22. Li L, Kang H, Zhang Q, D'Agati VD, Al-Awqati Q, Lin FM. FoxO3 activation in hypoxic tubules prevents chronic kidney disease. *J Clin Invest.* 2019;129:2374–89.
23. Baumann B, Hayashida T, Liang X, Schnaper HW. Hypoxia-inducible factor-1 $\alpha$  promotes glomerulosclerosis and regulates COL1A2 expression through interactions with Smad3. *Kidney Int.* 2016;90:797–808.
24. Tang TT, Lv LL, Wang B, Cao JY, Feng Y, Li ZL, et al. Employing macrophage-derived microvesicle for kidney-targeted delivery of dexamethasone: an efficient therapeutic strategy against renal inflammation and fibrosis. *Theranostics.* 2019;9:4740–55.
25. Liu D, Wen Y, Tang TT, Lv LL, Tang RN, Liu H, et al. Megalin/Cubulin-lysosome-mediated albumin reabsorption is involved in the tubular cell activation of NLRP3 inflammasome and tubulointerstitial inflammation. *J Biol Chem.* 2015;290:18018–28.
26. Chan MC, Iltott NE, Schödel J, Sims D, Tumber A, Lippl K, et al. Tuning the transcriptional response to hypoxia by inhibiting hypoxia-inducible factor (HIF) prolyl and asparaginyl hydroxylases. *J Biol Chem.* 2016;291:20661–73.
27. Li ZL, Lv LL, Wang B, Tang TT, Feng Y, Cao JY, et al. The profibrotic effects of MK-8617 on tubulointerstitial fibrosis mediated by the KLF5 regulating pathway. *FASEB J.* 2019;33:12630–43.
28. Koivunen P, Hirsilä M, Günzler V, Kivirikko KI, Myllyharju J. Catalytic properties of the asparaginyl hydroxylase (FIH) in the oxygen sensing pathway are distinct from those of its prolyl 4-hydroxylases. *J Biol Chem.* 2004;279:9899–904.
29. Sawhney S, Marks A, Fluck N, Levin A, McLernon D, Prescott G, et al. Post-discharge kidney function is associated with subsequent ten-year renal progression risk among survivors of acute kidney injury. *Kidney Int.* 2017;92:440–52.
30. Shu SQ, Wang Y, Zheng ML, Liu Z, Cai J, Tang C, et al. Hypoxia and hypoxia-inducible factors in kidney injury and repair. *Cells.* 2019;8:207.
31. Bracken CP, Fedele AO, Linke S, Balrak W, Lisy K, Whitelaw ML, et al. Cell-specific regulation of hypoxia-inducible factor (HIF)-1 $\alpha$  and HIF-2 $\alpha$  stabilization and transactivation in a graded oxygen environment. *J Biol Chem.* 2006;281:22575–85.
32. Dayan F, Roux D, Brahimi-Horn MC, Pouyssegur J, Mazure NM. The oxygen sensor factor-inhibiting hypoxia-inducible factor-1 controls expression of distinct genes through the bifunctional transcriptional character of hypoxia-inducible factor-1 $\alpha$ . *Cancer Res.* 2006;66:3688–98.
33. Chen WC, Lin HH, Tang MJ. Matrix-stiffness-regulated inverse expression of Krüppel-like factor 5 and Krüppel-like factor 4 in the pathogenesis of renal fibrosis. *Am J Pathol.* 2015;185:2468–81.
34. Shindo T, Manabe I, Fukushima Y, Tobe K, Aizawa K, Miyamoto S, et al. Krüppel-like Zinc-finger transcription factor KLF5/BTEB2 is a target for angiotensin II signaling and an essential regulator of cardiovascular remodeling. *Nat Med.* 2002;8:856–63.
35. Kushida N, Nomura S, Mimura I, Fujita T, Yamamoto S, Nangaku M, et al. Hypoxia-inducible factor-1 $\alpha$  activates the transforming growth factor- $\beta$ /SMAD3 pathway in kidney tubular epithelial cells. *Am J Nephrol.* 2016;44:276–85.
36. Nayak BK, Shanmugasundaram K, Friedrichs WE, Cavaglieri RC, Patel M, Barnes J, Block K. HIF-1 mediates renal fibrosis in OVE26 type 1 diabetic mice. *Diabetes.* 2016;65:1387–97.
37. Wilkins SE, Abboud MI, Hancock RL, Schofield CJ. Targeting protein-protein interactions in the HIF system. *ChemMedChem* 2016;11:773–86.
38. Tal R, Shaish A, Bangio L, Peled M, Breitbart E, Harats D. Activation of C-transactivation domain is essential for optimal HIF-1 $\alpha$ -mediated transcriptional and angiogenic effects. *Microvasc Res.* 2008;76:1–6.
39. Yeh TL, Leissing TM, Abboud MI, Thinnis CC, Atasoylu O, Holt-Martyn JP, et al. Molecular and cellular mechanisms of HIF prolyl hydroxylase inhibitors in clinical trials. *Chem Sci.* 2017;8:7651–68.
40. Maxwell PH, Eckardt KU. HIF prolyl hydroxylase inhibitors for the treatment of renal anaemia and beyond. *Nat Rev Nephrol.* 2016;12:157–68.